

1 Establishment of a reverse genetics system for SARS-CoV-2 using circular polymerase extension 2 reaction

3
4 Shiho Torii¹, Chikako Ono¹, Rigel Suzuki¹, Yuhei Morioka¹, Itsuki Anzai¹, Yuzy Fauzyah¹, Yusuke Maeda¹,
5 Wataru Kamitani², Takasuke Fukuhara^{1,3*}, and Yoshiharu Matsuura^{1*}
6

7 ¹Department of Molecular Virology, Research Institute for Microbial Diseases, Osaka University, Suita,
8 Japan, ²Department of Infectious Diseases and Host Defense, Graduate School of Medicine, Gunma
9 University, Maebashi, Japan, ³Department of Microbiology, Hokkaido University Graduate School of
10 Medicine, Sapporo, Japan

11 *Correspondence: T.F. (fukut@pop.med.hokudai.ac.jp) and Y.M. (matsuura@biken.osaka-u.ac.jp)
12

13 Summary

14 Severe acute respiratory syndrome coronavirus 2 (SARS-CoV-2) has been identified as the causative agent
15 of coronavirus disease 2019 (COVID-19). While the development of specific treatments and a vaccine is
16 urgently needed, functional analyses of SARS-CoV-2 have been limited by the lack of convenient
17 mutagenesis methods. In this study, we established a PCR-based, bacterium-free method to generate
18 SARS-CoV-2 infectious clones. Recombinant SARS-CoV-2 could be rescued at high titer with high
19 accuracy after assembling 10 SARS-CoV-2 cDNA fragments by circular polymerase extension reaction
20 (CPER) and transfection of the resulting circular genome into susceptible cells. Notably, the construction of
21 infectious clones for reporter viruses and mutant viruses could be completed in two simple steps:
22 introduction of reporter genes or mutations into the desirable DNA fragments (~5,000 base pairs) by PCR
23 and assembly of the DNA fragments by CPER. We hope that our reverse genetics system will contribute to
24 the further understanding of SARS-CoV-2.
25

26 Main text

27 Severe acute respiratory syndrome coronavirus 2 (SARS-CoV-2) in the genus *Betacoronavirus* in the
28 family *Coronaviridae* is the causative agent of a global pandemic of severe respiratory disease, coronavirus
29 disease 2019 (COVID-19)(Gorbalenya *et al.*, 2020). The virus was initially discovered in Wuhan, China, in
30 late December 2019 (Zhu *et al.*, 2020; Zou *et al.*, 2020; Wu *et al.*, 2020) and has spread worldwide. As of
31 August 26, 2020, more than 20 million COVID-19 cases have been confirmed in over 180 countries, and
32 more than 0.8 million deaths have been reported (<https://covid19.who.int/>). The development of effective
33 vaccines and specific treatments is necessary to overcome the current COVID-19 pandemic. To develop
34 effective antivirals and safety vaccines against SARS-CoV-2, further understanding of the proliferation and
35 pathogenesis of SARS-CoV-2 is needed. Although a large number of papers have been published since the
36 emergence of SARS-CoV-2, neither the functions of the viral proteins nor the molecular mechanisms of
37 propagation and pathogenesis of SARS-CoV-2 have been fully characterized. The development of a simple
38 and efficient reverse genetics system is urgently needed for further molecular studies of SARS-CoV-2.

39 While a variety of infectious clones harboring the full-length viral cDNA under suitable promoters in
40 the plasmid have been established, the plasmid system is not available for coronaviruses because of the
41 large size of their viral genomes [-30 kilobases (kb)]. Instead, bacterial artificial chromosomes (BAC) or in
42 vitro ligation of viral cDNA fragments have been classically utilized (Almazán *et al.*, 2006; Yount *et al.*,
43 2003; Scobey *et al.*, 2013; Terada *et al.*, 2019). Although these systems have allowed us to conduct
44 molecular studies of coronaviruses, they also have some disadvantages, particularly when performing
45 mutagenesis. In the case of BAC, undesired mutations, such as deletions or insertions, can be introduced
46 during bacterial amplification, and verification of the full-length genome every time is time-consuming.
47 Moreover, the in vitro ligation method is complicated and requires specific skills. Given these facts, it
48 seems difficult to rapidly introduce reporter genes or multiple mutations into viral genes by the classical
49 methods.

50 Recently, a method for the rapid generation of flavivirus infectious clones by circular polymerase
51 extension reaction (CPER) was reported (Edmonds *et al.*, 2013). In this approach, cDNA fragments
52 covering the full-length viral genome and a linker fragment, which encodes the promoter, polyA signal and
53 ribozyme sequence, are amplified by PCR. Because the amplified fragments are designed to include
54 overlapping ends with adjacent fragments, the amplified fragments can be extended as a circular viral
55 genome with a suitable promoter by an additional PCR using the amplified fragments. By direct
56 transfection of the circular viral genome with the promoter into susceptible cells, infectious viruses can be
57 recovered. This means that infectious clones of flaviviruses can be constructed without any bacterial
58 amplification or in vitro ligation. Using this CPER method, multiple reporter flaviviruses and chimeric

59 flaviviruses have been constructed (Tamura *et al.*, 2018; Piyasena *et al.*, 2019), and a variety of mutant
60 flaviviruses were easily generated and analyzed at the same time (Setoh *et al.*, 2019). These studies showed
61 that CPER is an effective approach for the characterization of viral proteins.

62 In this study, we tried to establish a CPER method for the construction of SARS-CoV-2 recombinants
63 possessing reporter genes and mutations. In addition, we compared the biological characteristics of the
64 recombinants rescued by the CPER method with the parental SARS-CoV-2.

65 First, we examined whether the CPER approach would be applicable for the construction of an
66 infectious clone of SARS-CoV-2. For this purpose, we used the SARS-CoV-2 strain HuDPKng19-020,
67 which was provided by Dr. Sakuragi at the Kanagawa Prefectural Institute of Public Health. A total of 10
68 viral gene fragments (G1 to G10) covering the entire genome of SARS-CoV-2, and a UTR linker fragment
69 encoding the sequences of the 3' 43 nt of SARS-CoV-2, hepatitis delta virus ribozyme (HDVr), bovine
70 growth hormone (BGH) polyA signal, cytomegalovirus (CMV) promoter and the 5' 25 nt of SARS-CoV-2,
71 were cloned into plasmids. Then, cDNA fragments of F1 to F10 and the UTR linker, possessing
72 complementary ends with 25 to 452 overlapping nucleotides, were amplified with specific primers and
73 subjected to CPER as templates (Figure 1A and Table S1). The cDNA fragments of F9 and F10 were
74 connected to F9/10 before CPER by overlap PCR. A negative control was prepared by CPER using cDNA
75 fragments excluding F9/10. The full-length cDNA clone of SARS-CoV-2 under the CMV promoter
76 obtained by CPER (condition 1 described in Star methods) was directly transfected into either BHK-21
77 cells or tetracycline-inducible ACE2 and TMPRSS2-expressing IFNAR1-deficient HEK293
78 (HEK293-3P6C33) cells without any purification steps. Because the SARS-CoV-2 nucleocapsid protein
79 was reported to enhance the propagation of coronavirus RNA transcripts (Xie *et al.*, 2020), the
80 nucleocapsid-expressing plasmid was transfected together with the CPER products into cells. Upon the
81 induction of ACE2 and TMPRSS2 expression in HEK293-3P6C33 cells or the overlaying of Vero cells
82 expressing TMPRSS2 (VeroE6/TMPRSS2) onto BHK-21 cells, propagation of SARS-CoV-2 was assessed
83 by cytopathic effects (CPE).

84 At 7 days post-transfection (dpt), CPE were observed in HEK293-3P6C33 cells transfected with the
85 CPER product (CPER PC), but not in those transfected with the negative control (CPER NC) (Figure 1B).
86 CPE was not observed in BHK-21 cells until 14 dpt of the CPER products (data not shown). Propagation of
87 the progeny viruses was examined by serial passages of the culture supernatants of HEK293-3P6C33 cells
88 in VeroE6/TMPRSS2 cells for 2 rounds. CPE were observed at 1 day post-infection (dpi) of the viruses of
89 both Passage 1 (P1) and P2 (data not shown). Infectious titers of the culture supernatants of
90 HEK293-3P6C33 cells at 7 dpt (P0), P1 and P2 viruses, collected at 2 dpi to VeroE6/TMPRSS2 cells, were
91 determined by 50% tissue culture infective dose (TCID₅₀) assays. The infectious titers of the P0, P1, and P2
92 viruses were 10^{5.8}, 10^{6.3}, and 10^{5.8} TCID₅₀/ml, respectively (data not shown), demonstrating that infectious
93 SARS-CoV-2 was rescued at high titer upon transfection of the CPER product into HEK293-3P6C33 cells,
94 and the recovered viruses were capable of propagating well in VeroE6/TMPRSS2 cells.

95 To optimize the conditions of recovery of infectious SARS-CoV-2 particles by CPER, the reactions
96 were performed using different numbers of cycles, steps and extension times (conditions 1 to 3 in Star
97 Methods). To investigate the effect of expression of nucleocapsid as shown previously (Xie *et al.*, 2020) on
98 the recovery of infectious particles, CPER products were transfected into HEK293-3P6C33 cells with or
99 without an expression plasmid of the nucleocapsid protein. Culture supernatants of HEK293-3P6C33 cells
100 transfected with the CPER product were collected at the indicated time points for 9 days, and infectious
101 titers were determined as the TCID₅₀. In cells transfected with the CPER products without F9/10 (CPER
102 NC), no CPE and no infectious titer in the supernatants was detected until 9 dpt (condition 3 without the
103 expression plasmid of the nucleocapsid protein is shown in Figure S1A). On the other hand, infectious
104 titers were detected from 5 dpt and reached around 10^{7.0} TCID₅₀/ml in the supernatants of cells transfected
105 with the CPER products, regardless of the reaction conditions (condition 3 without the expression plasmid
106 of the nucleocapsid protein is shown in Figure S1A). No effect of the expression of nucleocapsid protein
107 was observed, suggesting that nucleocapsid is not necessary to recover infectious particles in this method.
108 We selected condition 3 (an initial 2 minutes of denaturation at 98°C; followed by 35 cycles of 10 seconds
109 at 98°C, 15 seconds at 55°C, and 15 minutes at 68°C; and a final extension for 15 minutes at 68°C) for
110 further CPER to generate an infectious cDNA clone for the recovery of infectious particles after
111 transfection into HEK293-3P6C33 cells. Condition 3 was chosen because CPE appeared in cells at 5 dpt of
112 CPER products obtained by condition 3, but at 7 dpt of those obtained by conditions 1 and 2 (data not
113 shown).

114 To determine the full-length genome sequences of viruses recovered by the CPER method, 2 viruses (#1
115 and #2 in Table S2), which were obtained independently at different time points from the supernatants of
116 HEK293-3P6C33 cells, were passaged two times in VeroE6/TMPRSS2 cells, and subjected to Sanger

117 sequence analysis with specific primers. Sequence analyses of P0–P2 viruses demonstrated that the
118 recombinant viruses maintained genetic markers (two silent mutations, A7486T and T7489A; Figure 1C),
119 indicating that there was no contamination of parental virus. Importantly, except for the genetic markers,
120 there was only one difference (T to T/A) in all tested P0 viruses, suggesting that the reverse genetic system
121 for SARS-CoV-2 by CPER had high accuracy. While a large deletion occurred in P1 and P2 of the #2 virus,
122 that deletion was reported to occur during passage in Vero E6 cells (Lau *et al.*, 2020).

123 Next, we investigated the growth kinetics of recombinant viruses in comparison with parental
124 SARS-CoV-2. Recombinant viruses, which were recovered at 7 dpt of CPER products into
125 HEK293-3P6C33 cells, and parental SARS-CoV-2 were infected into VeroE6/TMPRSS2 cells at
126 multiplicities of infection (MOIs) of 0.001 and 0.01. Infectious titers in the culture supernatants of
127 VeroE6/TMPRSS2 cells were determined for 48 hours. Although the rescued viruses by CPER (CPER)
128 exhibited lower titers than the parental viruses (Original isolate) at 24 and 36 hours post-infection (hpi), no
129 significant difference in maximum titers was observed between the rescued and parental viruses (Figure
130 1D). These results suggest that propagation of the rescued SARS-CoV-2 by CPER is slow but reached
131 levels similar to those reached by the parental virus, as previously reported (Xie *et al.*, 2020). To examine
132 the viral RNA synthesis of the rescued viruses, Northern blot analyses were performed. In total, eight
133 subgenomic RNAs were detected in cells infected with both parental and rescued viruses, and all eight
134 RNAs were similar in size (Figure 1E). Taken together, these results showed that SARS-CoV-2 rescued by
135 the CPER method exhibits biological characteristics similar to those of the parental virus.

136 Next, we applied the CPER method for construction of recombinant SARS-CoV-2 carrying reporter
137 genes. The nucleotide sequences from 27,433 to 27,675 in ORF7 were replaced by the sfGFP gene, as
138 previously reported (Thi Nhu Thao *et al.*, 2020) (Figure 2A). Using the DNA fragments containing the
139 sfGFP gene, infectious DNA clones were assembled by CPER. CPE was observed in HEK293-3P6C33
140 cells at 7 dpt of CPER product, and the insertion of the reporter genes in the viruses recovered in the
141 culture supernatants was confirmed by Sanger sequence analysis (data not shown). Then, the wild-type
142 (WT) virus and sfGFP-carrying virus (GFP virus) were infected to VeroE6/TMPRSS2 cells at an MOI of
143 0.001 and the growth kinetics of the viruses were evaluated. GFP viruses exhibited lower titers than WT
144 viruses at the indicated time points and the maximum titers of GFP viruses at 36 hpi were significantly
145 lower than those of WT viruses at 48 hpi (Figure 2B). We also examined the expression of GFP in
146 Vero-TMPRSS2 cells upon infection with the GFP recombinant from 12 to 36 hpi by fluorescence
147 microscopy. The numbers of GFP-positive cells were increased from 12 to 36 hpi and almost all cells
148 exhibited the fluorescent signals at 24 and 36 hpi (Figure 2C). These results indicate that recombinant
149 SARS-CoV-2 harboring reporter genes could be quickly engineered by the CPER method and the GFP
150 viruses demonstrated lower growth kinetics than the WT viruses.

151 We also employed NanoLuc binary technology (NanoBiT) (Dixon *et al.*, 2016) in this study. NanoBiT
152 is a split reporter consisting of 2 subunits, high-affinity NanoBiT (HiBiT) (Schwinn *et al.*, 2018) and large
153 NanoBiT (LgBiT). By interaction of HiBiT and LgBiT in cells or in vitro, NanoLuc enzymatic activity can
154 be detected. Because a reporter virus can be generated by inserting a small cDNA fragment encoding 11
155 amino acids into the viral genome, the effect on viral growth and pathogenicity has been shown to be
156 minimum (Tamura *et al.*, 2018). In this study, we inserted a HiBiT luciferase gene (VSGWRLFKKIS) and
157 a linker sequence (GSSG) into the N terminus of the ORF6 gene of SARS-CoV-2 (Figure 2A) by overlap
158 PCR using DNA fragment F9 and specific primer sets (see Star Methods for details), and the recombinant
159 SARS-CoV-2 possessing HiBiT was generated by CPER using the resulting fragments. We confirmed the
160 incorporation of the HiBiT gene into the recombinant viruses by Sanger sequence analysis (Figure S1B).
161 Infectious titers in the culture supernatants of VeroE6/TMPRSS2 cells infected with the HiBiT
162 recombinants (ORF6-HiBiT) were comparable to those in the culture supernatants of the same cells
163 infected with the WT (Figure 2D). Luciferase activities in cells infected with the recombinant, as assessed
164 by addition of LgBiT protein into the cell lysates, were increased from 12 to 48 hpi (Figure 2E). These
165 results suggest that recombinant SARS-CoV-2 carrying HiBiT could be easily generated by overlap PCR
166 for introduction of HiBiT into the indicated places, followed by CPER to assemble the resulting DNA
167 fragments, which function as reporter viruses exhibiting growth kinetics comparable to the WT virus.

168 Finally, we examined whether the CPER method can be applied for the construction of recombinant
169 SARS-CoV-2 with the desired mutations. Substitution of D614 to G on the spike protein was frequently
170 detected, and became dominant in European, South and North American countries (Koyama *et al.*, 2020)
171 (<https://www.gisaid.org/epiflu-applications/hcov-19-genomic-epidemiology/>). To evaluate the effect of this
172 substitution on virus propagation, we introduced this mutation in fragment F8 of SARS-CoV-2 (strain
173 HuDPKng19-020), and generated the infectious clone by the CPER method. We confirmed the substitution
174 in the recombinant by Sanger sequence analysis (data not shown), but there was no difference in growth

175 kinetics between the WT and D614G recombinant in VeroE6/TMPRSS2 cells (Figure 2F). Collectively,
176 these results suggest that our novel reverse genetic system based on CPER is an efficient method for quick
177 generation of recombinants for SARS-CoV-2.

178 Reverse genetics is one of the essential tools to analyze the functions of viral proteins; however, due to
179 the large size of the coronavirus genome, gene manipulations for coronaviruses have been performed by
180 only a very limited number of groups. Here, we established a simple and quick reverse genetics system for
181 SARS-CoV-2 based on the CPER method. The system consists of two steps—namely, amplification of
182 fragments encoding promoter and viral genes, followed by assembly into infectious cDNA clones by PCR
183 without any bacterial amplification. Recombinant viruses were generated with high titers at 7 dpt of CPER
184 products into cells. Using high-fidelity polymerase, SARS-CoV-2 could be rescued with high accuracy, and
185 the rescued virus exhibited characteristics similar to those of the parental virus. It is worth noting that the
186 same tools, i.e., primers and promoter fragments, can be used for generation of viruses possessing multiple
187 mutations or reporters. This method will allow us to conduct high-throughput mutagenesis of SARS-CoV-2,
188 to clarify the function of viral proteins and the mechanisms of propagation and pathogenesis.

189 In this study, we first report that the CPER method is available to assemble a large size genome (30 kb)
190 of SARS-CoV-2 with high accuracy. While infectious clones were recovered by all CPER conditions we
191 examined, recombinant viruses were recovered only in HEK293-3P6C33 cells (Figure 1B), indicating that
192 the transfection efficiency of the CPER product and replication efficiency of viruses might be important to
193 produce recombinant viruses. Multiple primer sets for the generation of DNA fragments (F1–F10) were
194 examined (data not shown); however, recombinant viruses were recovered only when using the fragments
195 generated by the indicated primer sets (Table S1). As each SARS-CoV-2 subgenomic RNA contains a
196 common leader sequence (72 nucleotides) at the 5' end (Kim *et al.*, 2020), the design of optimal primer sets
197 seemed to be important for efficient assembly of the circular genome. In the case of the CPER method for
198 flaviviruses, it was reported that insect-specific flaviviruses, which can replicate only in insect-derived cells,
199 could be rescued using mosquito-derived C6/36 cells by replacing the CMV promoter with the OpIE2
200 promoter gene in the UTR linker fragment (Piyasena *et al.*, 2017). Deletion of 23 nucleotides in the 3'
201 region of the promoter, enhanced the efficiency of recovery of insect-specific flaviviruses (Piyasena *et al.*,
202 2017). In that sense, further investigation of the CPER conditions (i.e., promoter sequences and primer sets)
203 for SARS-CoV-2 may enhance the recovery of recombinants, even for slowly growing viruses. Moreover,
204 it might be possible to generate other coronaviruses and chimeric coronaviruses by using susceptible cell
205 lines and optimal promoters.

206 While the GFP recombinant virus exhibited a lower titer than the WT viruses, the HiBiT recombinants
207 exhibited growth kinetics similar to that of the WT virus, suggesting that the HiBiT virus might be suitable
208 for functional analyses. As we previously showed, HiBiT recombinant viruses could be useful for drug
209 screening and animal experiments (Tamura *et al.*, 2019; Tamura *et al.*, 2018). By combining the reporter
210 assay and mutational scanning, we were able to investigate the biological features of viral proteins of
211 SARS-CoV-2.

212 To generate avirulent strain for use in developing a safe live-attenuated vaccine for SARS-CoV-2, the
213 CPER method is very useful. To characterize escape mutants occurring through the use of antiviral drugs or
214 vaccinations, CPER can be a robust tool. In comparison with previous reverse genetics systems for
215 coronaviruses, the CPER method is easier and quicker, especially when applied for mutagenesis. We
216 believe that this method will be widely utilized in order to investigate SARS-CoV-2 and further clarify its
217 pathogenesis and propagation.

218

219 **Acknowledgements**

220 We thank M. Tomiyama for her secretarial work and M. Ishibashi, and K. Toyoda, for their technical
221 assistance. We also thank J. Sakuragi in Kanagawa Prefectural Institute of Public Health for providing
222 SARS-CoV-2. This work was supported from the Ministry of Health, Labor and Welfare of Japan and the
223 Japan Agency for Medical Research and Development (AMED; <http://www.amed.go.jp/>) (JP20wm0225002,
224 JP20he0822006, JP20fk0108264, JP20he0822008, JP20wm0225003, JP20fk0108267, JP19fk0108113, and
225 JP20wm0125010), and the Japan Society for the Promotion of Science KAKENHI (JP19K24679). S. Torii
226 is supported by a JSPS Research Fellowships for young scientists (<https://www.jsps.go.jp/english/e-grants/>)
227 (19J12641).

228

229 **We have no conflicts of interest to declare.**

230

231 **Author contributions**

232 S.T. performed all experiments and analyzed the data under the supervision of T.F. and Y.M. (Matsuura);

233 C.O., R.S., Y.M. (Morioka), I.A., Y.F., W.K., and Y.M. (Maeda) provided critical resources and scientific
234 insights; S.T. and T.F. wrote the original draft; C.O., R.S., Y.M. (Morioka), I.A., Y.F., W.K., Y.M. (Maeda),
235 and Y.M. (Matsuura) wrote, reviewed, and edited the final manuscript.

236

237 **Figure 1.**

238 **Establishment of CPER-based reverse genetics for SARS-CoV-2.**

239 (A) Schematic representation of a CPER approach for the generation of recombinant SARS-CoV-2. A total
240 of 9 fragments (F1 to F8, and F9/10) covering the full-length of the SARS-CoV-2 genome were amplified,
241 then assembled with a UTR linker fragment including the HDVr, the BGH polyA signal and the CMV
242 promoter by CPER. The resulting CPER products were transfected into the susceptible cells. (B)
243 HEK293-3P6C33 cells were transfected with the CPER product and the bright field image was acquired at
244 7 days post-transfection (dpt) (left). As a negative control, the CPER product obtained without fragment
245 F9/10 was transfected into cells and the bright field image was obtained at 7 dpt (right). (C) Genetic
246 markers (2 silent mutations, A7,486T and T7,489A) in the recombinant SARS-CoV-2 genome. (D)
247 Comparison of the growth kinetics of the recombinant SARS-CoV-2 generated by CPER with that of the
248 original isolate. VeroE6/TMPRSS2 cells were infected with the viruses (MOI=0.001 or 0.01), and
249 infectious titers in the culture supernatants of the SARS-CoV-2-infected cells were determined by TCID₅₀
250 assay from 12 to 48 hours post-infection (hpi). (E) Northern blot analyses of subgenomic RNAs. RNAs
251 extracted from cells infected with the parental virus and the recombinant SARS-CoV-2 recovered by CPER
252 were subjected to Northern blot analyses.

253

254 **Figure 2.**

255 **Characterization of SARS-CoV-2 recombinants possessing reporter genes and mutations.**

256 (A) Gene structure of recombinant SARS-CoV-2 carrying the sfGFP or HiBiT gene. The nucleotide
257 sequences of 27,433–27,675 in ORF7 were replaced with those of sfGFP. The HiBiT gene was inserted into
258 the N terminus of ORF6. (B) Growth kinetics of wild-type SARS-CoV-2 (WT) and SARS-CoV-2 carrying
259 sfGFP (GFP). VeroE6/TMPRSS2 cells were infected with the viruses (MOI=0.001), and infectious titers in
260 the culture supernatants were determined at the indicated time points. (C) The fluorescent signal in
261 VeroE6/TMPRSS2 cells infected with the WT virus and GFP virus was observed for 36 hpi. (D) Growth
262 kinetics of the WT virus and recombinant virus possessing the HiBiT gene in ORF6 (ORF6-HiBiT). Titers
263 in the culture supernatants of VeroE6/TMPRSS2 cells, infected with the viruses (MOI=0.01), were
264 measured for 48 hours. (E) Luciferase activities in VeroE6/TMPRSS2 cells infected with the WT virus and
265 ORF6-HiBiT virus were determined from 12 to 48 hpi. (F) Infectious titers in the culture supernatants of
266 VeroE6/TMPRSS2 cells infected with the WT virus or mutant virus, harboring a substitution of D614 to G
267 in the spike protein (D614G), were determined at the indicated time points.

268

269 **Star methods**

270 **Lead Contact**

271 Further information and requests for resources and reagents should be directed to and will be fulfilled by
272 either of the two Lead Contacts, Takasuke Fukuhara (fukut@pop.med.hokudai.ac.jp) or Yoshiharu
273 Matsuura (matsuura@biken.osaka-u.ac.jp).

274

275 **Materials Availability**

276 All unique materials generated in this study are available from either of the two lead contacts with a
277 completed Materials Transfer Agreement.

278

279 **Data Code and Availability**

280 This study did not generate any unique datasets or code.

281

282 **Experimental Model and Subject details**

283 **Viruses and Cells**

284 SARS-CoV-2 strain HuDPKng19-020 was kindly provided by Dr. Sakuragi at the Kanagawa Prefectural
285 Institute of Public Health. All viruses were initially amplified in Vero E6 cells and the culture supernatants
286 were harvested and stored at -80°C until use. BHK-21 cells and Vero E6 cells were maintained in
287 high-glucose Dulbecco's Modified Eagle Medium (DMEM) (Nacalai Tesque) containing 10% fetal bovine
288 serum (FBS) (Sigma), 100 units/ml penicillin and 100 µg/ml streptomycin (P/S) (Sigma).
289 TMPRSS2-expressing Vero E6 (VeroE6/TMPRSS2) cells were obtained from the Japanese Collection of
290 Research Bioresources Cell Bank (JCRB1819), and maintained in DMEM containing 10% FBS and G418

291 (Nacalai Tesque). IFNAR1-deficient HEK293 cells, in which human ACE2 and TMPRSS2 are induced by
292 tetracycline, were established and designated as HEK293-3P6C33 cells. In brief, ACE2 carboxyl terminally
293 tagged with BFP followed by IRES-TMPRSS2 was constructed under a tetracycline-responsive promoter
294 in a piggyback-based vector (Yusa *et al.*, 2009) (kindly provided from Wellcome Trust Sanger Institute).
295 EF-1alpha-driven rtTA-P2A-bsd was also inserted into this vector. Then, this plasmid was co-transfected
296 with a transposase-expression vector, pCMV-hyPBBase (Yusa *et al.*, 2011) (kindly provided from Wellcome
297 Trust Sanger Institute), into HEK293 cells, whose IFNAR1 had been knocked out using a CRISPR/Cas9
298 system. The HEK293-3P6C33 cells were maintained in DMEM containing 10% FBS and Blasticidin
299 (solution) (10 µg/ml) (Invivogen), and the exogenous expression of ACE2 and TMPRSS2 was induced by
300 addition of doxycycline hydrochloride (1 µg/ml) (Sigma). All the above cells were cultured at 37°C under
301 5% CO₂. All experiments involving SARS-CoV-2 were performed in biosafety level-3 laboratories,
302 following the standard biosafety protocols approved by the Research institute for Microbial Diseases at
303 Osaka University.

304

305 **Method details**

306 **RNA extraction, cDNA synthesis, and determination of nucleotide sequences of the full-length 307 SARS-CoV-2 genome**

308 Total RNA was extracted from the supernatants of SARS-CoV-2-infected cells by using a PureLink RNA
309 Mini Kit (Invitrogen). Thereafter, first-strand cDNA was synthesized by using a PrimeScript RT reagent kit
310 (Perfect Real Time) (TaKaRa Bio) with random hexamer primers and extracted RNA, according to the
311 manufacturer's protocols. To determine the nucleotide sequences of full-length SARS-CoV-2, a total of 10
312 gene fragments (G1–G10), which are up to 4,000 base pairs in length and cover the entire SARS-CoV-2
313 sequence, were amplified with synthesized cDNA, specific primer sets for SARS-CoV-2 and PrimeSTAR
314 GXL DNA polymerase (TaKaRa Bio). The 5' termini of RNA were amplified by using the 5'RACE System
315 for Rapid Amplification of cDNA Ends, Version 2.0 (Thermo Fisher Scientific) with specific primers
316 (CoV-2-Race1 and CoV-2-Race2) as previously described (Li *et al.*, 2005). Then, the amplified products
317 were directly sequenced in both directions by using the ABI PRISM 3130 Genetic Analyzer (Applied
318 Biosystems) with specific primers.

319

320 **Plasmids**

321 A total of 10 SARS-CoV-2 (HuDPKng19-020) cDNA fragments (G1–G10) were amplified by PrimeSTAR
322 GXL DNA polymerase and cloned into plasmids. SARS-CoV-2 fragments (G1, G2, G3, G4, G7, G8, G9
323 and G10) were cloned into the lentiviral vector pCSII-EF-RfA (pCSII-CoV-2-G1, -G2, -G3, -G4, -G7, -G8,
324 -G9 and -G10), and other fragments (G5 and G6) were cloned into the pMW119 vector (pMW-CoV-2-G5
325 and -G6). A UTR linker for SARS-CoV-2 was also generated using the pMW119 vector, which encodes
326 sequences of the 3' 43 nt of SARS-CoV-2, BGH polyA signal, HDVr, CMV promoter and the 5' 25 nt of
327 SARS-CoV-2 (pMW-CoV-2-UTRlinker). To distinguish between the recombinant viruses and the original
328 virus, two silent mutations, A7,486T and T7,489A, were introduced into pCSII-CoV-2-G4 as genetic
329 markers. To generate reporter viruses possessing the sfGFP gene, the nucleotide sequences of 27,433–
330 27,675 in the ORF7 region in pCSII-CoV-2-G10 were replaced with the sfGFP gene as previously
331 described (Thi Nhu Thao *et al.*, 2020). The resulting vectors were designated as pCSII-CoV-2-G10-sfGFP.
332 A plasmid expressing the SARS-CoV-2 nucleocapsid was constructed by inserting the cDNA of the
333 nucleocapsid into pCAGGS (pCAGGS-CoV-2-N). Sequences of all the inserted DNAs were confirmed by
334 sequencing (ABI PRISM 3130 Genetic Analyzer).

335

336 **CPER reaction**

337 SARS-CoV-2 recombinants were generated by CPER as described previously (Setoh *et al.*, 2017), with
338 some modifications. To amplify all the cDNA fragments having complementary ends with a 25- to
339 452-nucleotide overlap for CPER, plasmids encoding SARS-CoV-2 gene fragments (G1–G10) and
340 UTRlinker were used as templates. The specific primers used to amplify DNA fragments (F1–F10 and the
341 UTR linker) are described in the Key resources table. Then, the DNA fragments of F9 and F10 were
342 connected before CPER by overlap PCR with a primer set (CoV-2-F9-Fw and CoV-2-F10-Rv). By using
343 equimolar amounts (0.1 pmol each) of the resulting 10 DNA fragments (F1 to F8, F9/10 and the UTR
344 linker) and 2 µl of PrimeStar GXL DNA polymerase, CPER was performed within 50 µl reaction volumes.
345 The cycling conditions of CPER were as follows: condition 1 (an initial 2 minutes of denaturation at 98°C;
346 20 cycles of 10 seconds at 98°C, 15 seconds at 55°C, and 25 minutes at 68°C; and a final extension for 25
347 minutes at 68°C), condition 2 (an initial 2 minutes of denaturation at 98°C; 35 cycles of 10 seconds at 98°C
348 and 15 minutes at 68°C; and a final extension for 15 minutes at 68°C), or condition 3 (an initial 2 minutes

349 of denaturation at 98°C; 35 cycles of 10 seconds at 98°C, 15 seconds at 55°C, and 15 minutes at 68°C; and
350 a final extension for 15 minutes at 68°C).

351 The infectious clones of SARS-CoV-2 carrying sfGFP were also assembled by CPER using
352 pCSII-CoV-2-G10-sfGFP as templates to acquire DNA fragment F10. The HiBiT recombinant
353 SARS-CoV-2 was also generated by CPER as previously described (Tamura *et al.*, 2018), with some
354 modifications. The HiBiT gene (VSGWRLFKKIS) and a linker sequence (GSSG) were inserted in the N
355 terminus of the ORF6 sequence by overlap PCR using DNA fragment F9 and a specific primer set
356 (ORF6-HiBiT-Rv and ORF6-HiBiT-Fw). Thereafter, CPER was conducted using the resulting fragment F9
357 containing the HiBiT gene.

358

359 **Transfection**

360 The CPER products (25 µl out of a 50 µl reaction volume) were transfected into HEK293-3P6C33 cells or
361 BHK-21 cells with Trans IT LT-1 (Mirus), following the manufacturer's protocols. At 6 hours
362 post-transfection, the culture supernatants of HEK293-3P6C33 cells were replaced with DMEM containing
363 2% FBS and doxycycline hydrochloride (1 µg/ml), and BHK-21 cells were overlaid by VeroE6/TMPRSS2
364 cells.

365

366 **Titration and growth kinetics**

367 The infectious titers in the culture supernatants were determined by the 50% tissue culture infective doses
368 (TCID₅₀). The culture supernatants of cells were inoculated onto VeroE6/TMPRSS2 cells in 96-well plates
369 after ten-fold serial dilution with DMEM containing 2% FBS, and the infectious titers were determined at
370 72 hours post-infection (hpi). For growth kinetics, SARS-CoV-2 was inoculated into VeroE6/TMPRSS2
371 cells in 6-well plates at a multiplicity of infection (MOI) of 0.001 or 0.01 and the culture supernatants were
372 replaced with new media at 1 hpi and incubated for 48 hours. The infectious titers in the culture
373 supernatants of cells collected at 12, 24, 36 and 48 hpi were determined.

374

375 **Northern blotting**

376 Total RNAs were extracted from cells infected with the WT or recombinant SARS-CoV-2 and subjected to
377 northern blot analysis as previously described (Xie *et al.*, 2020). A digoxigenin (DIG)-labeled
378 random-primed probe, corresponding to 28,999 to 29,573 of the SARS-CoV-2 genome, was generated by
379 using a DIG RNA Labeling kit (SP6/T7) (Roche), and utilized to detect viral mRNAs. The RNAs were
380 washed with the DIG luminescent detection kit (Roche) and visualized with CDP-Star Chemiluminescent
381 Substrate (Roche), according to the manufacturer's protocols.

382

383 **HiBiT luciferase assay**

384 SARS-CoV-2 infected cells were collected at the indicated time points and subjected to luciferase assay.
385 Luciferase activity was measured by using a Nano-Glo HiBiT Lytic assay system (Promega), following the
386 manufacturer's protocols. In brief, the HiBiT assay was conducted by adding Nano-Glo substrate and
387 LgBiT protein into the lysates of cells infected with viruses, and then measuring the luciferase activities
388 with a luminometer.

389

390 **Statistical analysis and normalizing**

391 All assays were performed independently at least 2 times. The data were expressed as means ±S.D.
392 Statistical significance was determined by the two-tailed Student's *t*-test. *P*-values <0.05 were considered
393 significant and indicated by a single asterisk (*).

394

395 **The supplemental information includes 1 figure and 2 tables.**

396 **Figure S1. Characterization of recombinant SARS-CoV-2.**

397 (A) Time course analysis of infectious SARS-CoV-2 production. CPER products were transfected into
398 HEK293-3P6C33 cells (CPER PC), and infectious titers in the culture supernatants were measured at the
399 indicated time points. As a negative control, the CPER product obtained without fragment F9/10 was
400 transfected into cells (CPER NC). (B) Sequence analysis of the recombinant virus possessing the HiBiT
401 gene in ORF6. The HiBiT gene and a linker sequence were inserted into the N terminus of the ORF6
402 sequence.

403 **Table S1. SARS-CoV-2 DNA fragments used for CPER reaction**

404 **Table S2. Mutations of recombinant SARS-CoV-2 (P0–P2 viruses)**

405

406

407 **References**

- 408 Almazán, F., Dediego, M. L., Galán, C., Escors, D., Alvarez, E., Ortego, J., Sola, I., Zuñiga, S., Alonso, S.,
409 Moreno, J. L., et al. (2006) 'Construction of a severe acute respiratory syndrome coronavirus infectious
410 cDNA clone and a replicon to study coronavirus RNA synthesis', *J Virol*, 80(21), pp. 10900–10906.
- 411 Dixon, A. S., Schwinn, M. K., Hall, M. P., Zimmerman, K., Otto, P., Lubben, T. H., Butler, B. L.,
412 Binkowski, B. F., Machleidt, T., Kirkland, T. A., et al. (2016) 'NanoLuc Complementation Reporter
413 Optimized for Accurate Measurement of Protein Interactions in Cells', *ACS Chem Biol*, 11(2), pp. 400–408.
- 414 Edmonds, J., van Grinsven, E., Prow, N., Bosco-Lauth, A., Brault, A. C., Bowen, R. A., Hall, R. A. and
415 Khromykh, A. A. (2013) 'A novel bacterium-free method for generation of flavivirus infectious DNA by
416 circular polymerase extension reaction allows accurate recapitulation of viral heterogeneity', *J Virol*, 87(4),
417 pp. 2367–2372.
- 418 Gorbalenya, A. E., Baker, S. C., Baric, R. S., de Groot, R. J., Drosten, C., Gulyaeva, A. A., Haagmans, B.
419 L., Lauber, C., Leontovich, A. M., Neuman, B. W., et al. (2020) 'The species Severe acute respiratory
420 syndrome-related coronavirus: classifying 2019-nCoV and naming it SARS-CoV-2', *Nat Microbiol*, 5(4),
421 pp. 536–544.
- 422 Kim, D., Lee, J. Y., Yang, J. S., Kim, J. W., Kim, V. N. and Chang, H. (2020) 'The Architecture of
423 SARS-CoV-2 Transcriptome', *Cell*, 181(4), pp. 914–921.e10.
- 424 Koyama, T., Weeraratne, D., Snowden, J. L. and Parida, L. (2020) 'Emergence of Drift Variants That May
425 Affect COVID-19 Vaccine Development and Antibody Treatment', *Pathogens*, 9(5).
- 426 Lau, S. Y., Wang, P., Mok, B. W., Zhang, A. J., Chu, H., Lee, A. C., Deng, S., Chen, P., Chan, K. H., Song,
427 W., et al. (2020) 'Attenuated SARS-CoV-2 variants with deletions at the S1/S2 junction', *Emerg Microbes
428 Infect*, 9(1), pp. 837–842.
- 429 Li, Z., Yu, M., Zhang, H., Wang, H. Y. and Wang, L. F. (2005) 'Improved rapid amplification of cDNA
430 ends (RACE) for mapping both the 5' and 3' terminal sequences of paramyxovirus genomes', *J Virol
431 Methods*, 130(1–2), pp. 154–156.
- 432 Piyasena, T. B. H., Newton, N. D., Hobson-Peters, J., Vet, L. J., Setoh, Y. X., Bielefeldt-Ohmann, H.,
433 Khromykh, A. A. and Hall, R. A. (2019) 'Chimeric viruses of the insect-specific flavivirus Palm Creek with
434 structural proteins of vertebrate-infecting flaviviruses identify barriers to replication of insect-specific
435 flaviviruses in vertebrate cells', *J Gen Virol*, 100(11), pp. 1580–1586.
- 436 Piyasena, T. B. H., Setoh, Y. X., Hobson-Peters, J., Newton, N. D., Bielefeldt-Ohmann, H., McLean, B. J.,
437 Vet, L. J., Khromykh, A. A. and Hall, R. A. (2017) 'Infectious DNAs derived from insect-specific
438 flavivirus genomes enable identification of pre- and post-entry host restrictions in vertebrate cells', *Sci Rep*,
439 7(1), pp. 2940.
- 440 Schwinn, M. K., Machleidt, T., Zimmerman, K., Eggers, C. T., Dixon, A. S., Hurst, R., Hall, M. P., Encell,
441 L. P., Binkowski, B. F. and Wood, K. V. (2018) 'CRISPR-Mediated Tagging of Endogenous Proteins with
442 a Luminescent Peptide', *ACS Chem Biol*, 13(2), pp. 467–474.
- 443 Scobey, T., Yount, B. L., Sims, A. C., Donaldson, E. F., Agnihothram, S. S., Menachery, V. D., Graham, R.
444 L., Swanstrom, J., Bove, P. F., Kim, J. D., et al. (2013) 'Reverse genetics with a full-length infectious
445 cDNA of the Middle East respiratory syndrome coronavirus', *Proc Natl Acad Sci U S A*, 110(40), pp.
446 16157–16162.
- 447 Setoh, Y. X., Amarilla, A. A., Peng, N. Y. G., Griffiths, R. E., Carrera, J., Freney, M. E., Nakayama, E.,
448 Ogawa, S., Watterson, D., Modhiran, N., et al. (2019) 'Determinants of Zika virus host tropism uncovered
449 by deep mutational scanning', *Nat Microbiol*, 4(5), pp. 876–887.

450 Setoh, Y. X., Prow, N. A., Peng, N., Hugo, L. E., Devine, G., Hazlewood, J. E., Suhrbier, A. and
451 Khromykh, A. A. (2017) 'Generation and Characterization of New Zika Virus Isolate Using Sequence Data
452 from a Microcephaly Case', *mSphere*, 2(3).

453 Tamura, T., Fukuhara, T., Uchida, T., Ono, C., Mori, H., Sato, A., Fauzyah, Y., Okamoto, T., Kurosu, T.,
454 Setoh, Y. X., et al. (2018) 'Characterization of Recombinant Flaviviridae Viruses Possessing a Small
455 Reporter Tag', *J Virol*, 92(2).

456 Tamura, T., Igarashi, M., Enkhbold, B., Suzuki, T., Okamatsu, M., Ono, C., Mori, H., Izumi, T., Sato, A.,
457 Fauzyah, Y., et al. (2019) 'Dynamics of Reporter', *J Virol*, 93(22).

458 Terada, Y., Kuroda, Y., Morikawa, S., Matsuura, Y., Maeda, K. and Kamitani, W. (2019) 'Establishment of
459 a Virulent Full-Length cDNA Clone for Type I Feline Coronavirus Strain C3663', *J Virol*, 93(21).

460 Thi Nhu Thao, T., Labroussaa, F., Ebert, N., V'kovski, P., Stalder, H., Portmann, J., Kelly, J., Steiner, S.,
461 Holwerda, M., Kratzel, A., et al. (2020) 'Rapid reconstruction of SARS-CoV-2 using a synthetic genomics
462 platform', *Nature*, 582(7813), pp. 561–565.

463 Wu, F., Zhao, S., Yu, B., Chen, Y. M., Wang, W., Song, Z. G., Hu, Y., Tao, Z. W., Tian, J. H., Pei, Y. Y.,
464 Y, et al. (2020) 'A new coronavirus associated with human respiratory disease in China', *Nature*, 579(7798),
465 pp. 265–269.

466 Xie, X., Muruato, A., Lokugamage, K. G., Narayanan, K., Zhang, X., Zou, J., Liu, J., Schindewolf, C.,
467 Bopp, N. E., Aguilar, P. V., et al. (2020) 'An Infectious cDNA Clone of SARS-CoV-2', *Cell Host Microbe*,
468 27(5), pp. 841–848.e3.

469 Yount, B., Curtis, K. M., Fritz, E. A., Hensley, L. E., Jahrling, P. B., Prentice, E., Denison, M. R., Geisbert,
470 T. W. and Baric, R. S. (2003) 'Reverse genetics with a full-length infectious cDNA of severe acute
471 respiratory syndrome coronavirus', *Proc Natl Acad Sci U S A*, 100(22), pp. 12995–30000.

472 Yusa, K., Rad, R., Takeda, J. and Bradley, A. (2009) 'Generation of transgene-free induced pluripotent
473 mouse stem cells by the piggyBac transposon', *Nat Methods*, 6(5), pp. 363–369.

474 Yusa, K., Zhou, L., Li, M. A., Bradley, A. and Craig, N. L. (2011) 'A hyperactive piggyBac transposase for
475 mammalian applications', *Proc Natl Acad Sci U S A*, 108(4), pp. 1531–1536.

476 Zhu, N., Zhang, D., Wang, W., Li, X., Yang, B., Song, J., Zhao, X., Huang, B., Shi, W., Lu, R., et al.
477 (2020) 'A Novel Coronavirus from Patients with Pneumonia in China, 2019', *N Engl J Med*, 382(8), pp.
478 727–733.

479 Zou, L., Ruan, F., Huang, M., Liang, L., Huang, H., Hong, Z., Yu, J., Kang, M., Song, Y., Xia, J., et al.
480 (2020) 'SARS-CoV-2 Viral Load in Upper Respiratory Specimens of Infected Patients', *N Engl J Med*,
481 382(12), pp. 1177–1179.

482

483

Fig. 1 Torii et al.

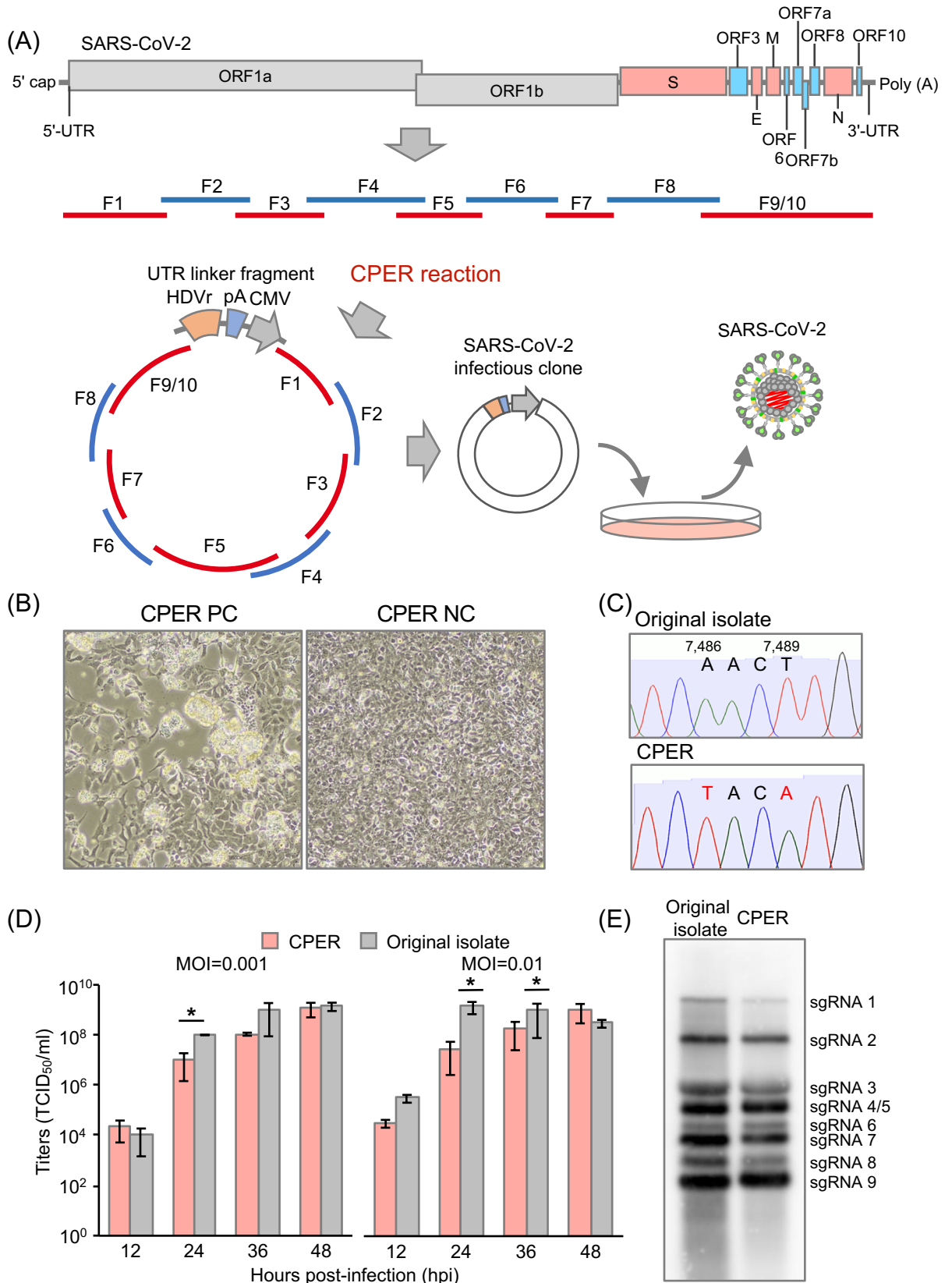


Fig. 2 Torii et al.

